Discrete crack modeling of RC structure using hybrid-type penalty method

***Y. Fujiwara[1], N. Takeuchi[1], T. Shiomi[2], and A. Kambayashi[3]**

[1]Graduate School of Engineering and Design, Hosei University, 2-33 Ichigaya Tamachi, Shinjuku, Tokyo, Japan.
[2]Mind Inc., 7-17-19 Maebara-nishi Funabashi Chiba, Japan.
[3] Research & Development Institute, Takenaka Corporation, 1-5-1 Ohtsuka, Inzai, Chiba, Japan.

*Corresponding author: fujiwara.yoshihiro@3d-lab.jp

Abstract

The hybrid-type penalty method (HPM) is suitable for representing failure phenomena that occur during the transition from continua to discontinua in materials such as concrete. The initiation and propagation of dominant cracks and the branching of cracks can easily be modeled as discrete cracks. The HPM represents a discrete crack by eliminating the penalty that represents the separation of elements at the intersection boundary. This treatment is easy because no change is required in the degrees of freedom for the discrete crack. In addition, it is important to correctly evaluate the deformation of continua before crack formation is initiated. To achieve this, we implemented a constitutive model of reinforced concrete for the HPM. In this paper, we present the implemented constitutive model and describe the simulation of a deep beam test using the HPM to demonstrate its capability for evaluating progressive failure.

Keywords: Hybrid-type penalty method, Discrete crack, Reinforced concrete

Introduction

Recent large earthquakes caused significant damage to concrete structures. Therefore, understanding the failure mechanism of concrete structures is important. A dominant crack is initiated in a concrete structure because of tensile stress. The crack subsequently grows, propagates, and branches until the structure finally collapses. To predict the progressive failure of a concrete structure, accurate computation of a discrete crack is essential. Computer simulations can predict the crack growth, propagation, and branching that lead to failure of the concrete structure.

The rigid body spring model (RBSM) developed by Kawai (1977) is a good method for modeling a discrete crack. The advantage of this method lies in its simplicity; there is no need to track the crack path. Initially, the model obtained good results when solving the problem of the strong nonlinearity of steel. It was then applied to discrete limit analysis of soils and concrete structures (Takeuchi et al., 2005). Unfortunately, the elastic deformation in continua obtained by the RBSM is not accurate because it models a continuum that connects the spring elements between the edges of rigid bodies. However, the RBSM is still used to model the realistic behavior of concrete structures, which includes cracking and failure (Gedik et al., 2011).

The hybrid-type penalty method (HPM) developed by Takeuchi et al. (2009) refined the RBSM method for calculating the elastic deformations of elements using the finite element method; a Lagrange multiplier was also introduced to satisfy the subsidiary condition of continuous displacement in the hybrid-type virtual work formulation. The HPM is suitable for analyzing the progressive failure of concrete structures; this method offers the following features:

- Accurate deformation can be calculated before crack initiation because an elastic element (called a subdomain in the HPM) is used. Even after crack initiation, accurately calculating the deformation within the elastic area between cracks is important.

- The HPM models a discrete crack by eliminating the penalty caused by separation of the elements at the intersection boundary. This treatment is easy because no change is required in the degrees of freedom for a discrete crack.

- The concentrated stress at the crack tip can be calculated without the use of the J-integral, which was originally developed by Rice (1968). The HPM can easily and accurately obtain

concentrated stresses around the crack by directly using the correct relationship between the tensile stress and displacement of the crack mouth opening. It can calculate not only the growth of the existing cracks but also the formation of new cracks.

We simulated an anchor bolt pullout test in plain concrete, and the results matched well with the experimental results (Fujiwara *et al*., 2012). As a next step, we implemented a constitutive model of a reinforcing bar in the HPM to allow for computation of the progressive failure phenomena of a reinforced concrete structure.

In the present paper, we introduce the basic formulation of the HPM and describe an implemented constitutive model of reinforced concrete. We validated the accuracy of the constitutive model by simulating a deep beam test.

Theory of HPM

Governing Equation

The basic equations of the elastic problem are as follows:

$$\operatorname{div} \boldsymbol{\sigma} + \boldsymbol{f} = 0 \quad \text{in } \Omega, \tag{1}$$

$$\boldsymbol{\sigma} = \boldsymbol{D} : \boldsymbol{\varepsilon}, \tag{2}$$

$$\boldsymbol{\varepsilon} = \boldsymbol{\nabla}^s \boldsymbol{u} \overset{\text{def.}}{=} \frac{1}{2}\left[\boldsymbol{\nabla}\boldsymbol{u} + (\boldsymbol{\nabla}\boldsymbol{u})^t\right], \tag{3}$$

where $\boldsymbol{\sigma}$ is the Cauchy stress tensor; $\boldsymbol{f}$ is the body force per unit volume; $\boldsymbol{\varepsilon}$ is the infinitesimal strain tensor; $\boldsymbol{D}$ is the constitutive tensor; $\nabla := (\partial/\partial x_i)\boldsymbol{e}_i$ is the differential operator; $\boldsymbol{\nabla}^s$ is the symmetric part of $\boldsymbol{\nabla}$; and $\boldsymbol{u}$ is the displacement field in $\boldsymbol{x} \in \Omega$, where Ω is the reference configuration of the continuum body with a smooth boundary $\Gamma = \Gamma_u \cup \Gamma_\sigma$. Here, $\Gamma_u := \partial_u\Omega \subset \partial\Omega$ is the geometric boundary, and $\Gamma_\sigma := \partial_\sigma\Omega \subset \partial\Omega$ is the stress boundary. At the boundaries, the following conditions are satisfied:

$$\boldsymbol{u}|_{\Gamma_u} = \hat{\boldsymbol{u}} \ \ (\text{given}), \tag{4}$$

$$\boldsymbol{\sigma}|_{\Gamma_\sigma}\, \boldsymbol{n} = \hat{\boldsymbol{t}} \ \ (\text{given}), \tag{5}$$

where $\boldsymbol{t}$ is the traction and $\boldsymbol{n}$ is the field normal to the boundary Γ_σ.

Let Ω consist of M subdomains $\Omega^{(e)} \subset \Omega$ with the closed boundary $\Gamma^{(e)} := \partial\Omega^{(e)}$, as shown in Fig. 1, that is,

$$\Omega = \bigcup_{e=1}^{M} \Omega^{(e)} \quad \text{where } \Omega^{(r)} \cap \Omega^{(q)} = 0 \quad (r \neq q). \tag{6}$$

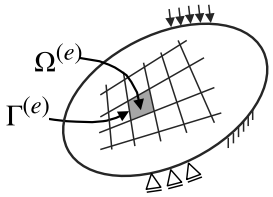

Figure 1. Subdomain $\Omega^{(e)}$ and its common boundary $\Gamma^{(e)}$

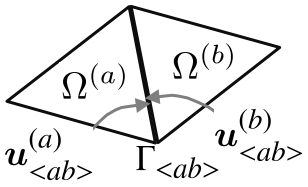

Figure 2. Boundary $\Gamma_{<ab>}$ between subdomains $\Omega^{(a)}$ and $\Omega^{(b)}$

We denote $\Gamma_{<ab>}$ as the common boundary between two subdomains $\Omega^{(a)}$ and $\Omega^{(b)}$, which are adjoined, as shown in Fig. 2; $\Gamma_{<ab>}$ is defined as follows:

$$\Gamma_{<ab>} \overset{\text{def.}}{=} \Gamma^{(a)} \cap \Gamma^{(b)}. \tag{7}$$

The relation for the displacement of $\Gamma_{<ab>}$, which is the intersection boundary between $\Omega^{(a)}$ and $\Omega^{(b)}$, is as follows:

$$\boldsymbol{u}^{(a)}_{<ab>} = \boldsymbol{u}^{(b)}_{<ab>} \quad \text{on } \Gamma_{<ab>}. \tag{8}$$

Equation (8) introduces a subsidiary condition into the framework of the virtual work equation with the Lagrange multiplier $\boldsymbol{\lambda}$ as follows:

$$H_{ab} \overset{\text{def.}}{=} \delta \int_{\Gamma_{<ab>}} \boldsymbol{\lambda}\cdot(\boldsymbol{u}^{(a)}_{<ab>} - \boldsymbol{u}^{(b)}_{<ab>})\, dS, \tag{9}$$

where $\delta(\bullet)$ represents the variation in $(\bullet)$. From Eqs. (1) and (9), the following hybrid-type virtual work equation is obtained (Mihara and Takeuchi, 2008):

$$\sum_{e=1}^{M}\left(\int_{\Omega^{(e)}} \boldsymbol{\sigma}:\mathrm{grad}(\delta\boldsymbol{u})dV - \int_{\Omega^{(e)}} \boldsymbol{f}\cdot\delta\boldsymbol{u}\, dV\right)$$
$$-\sum_{s=1}^{N}\left(\delta\int_{\Gamma_{<s>}} \boldsymbol{\lambda}\cdot(\boldsymbol{u}^{(s_a)}_{<s>} - \boldsymbol{u}^{(s_b)}_{<s>})\, dS\right) - \int_{\Gamma_\sigma} \hat{\boldsymbol{t}}\cdot\delta\boldsymbol{u}\, dS = 0\ {}^{\forall}\delta\boldsymbol{u}. \tag{10}$$

Here, N represents the number of common boundaries of the subdomain, and $\delta\boldsymbol{u}$ represents the virtual displacement. The superscripts (s_a) and (s_b) represent the subdomains $\Omega^{(s_a)}$ and $\Omega^{(s_b)}$, respectively, related to the common boundary $\Gamma_{<s>}$.

The physical interpretation of the Lagrange multiplier $\boldsymbol{\lambda}$ is that of a surface force at the boundary $\Gamma_{<s>}$. In this paper, the Lagrange multiplier $\boldsymbol{\lambda}_{<ab>}$ on the boundary $\Gamma_{<ab>}$ is defined as follows:

$$\boldsymbol{\lambda}_{<ab>} = \boldsymbol{k}\cdot\boldsymbol{\delta}_{<ab>}. \tag{11}$$

Here, $\delta_{<ab>}$ represents the relative displacement on the boundary $\Gamma_{<ab>}$, and $\boldsymbol{k}$ is the penalty function.

Discretized Equation in Matrix Form

The independent linear displacement field $\boldsymbol{u}^{(e)}$ in each subdomain $\Omega^{(e)}$ is assumed to be as follows:

$$\boldsymbol{u}^{(e)} = \boldsymbol{N}^{(e)}_d\boldsymbol{d}^{(e)} + \boldsymbol{N}^{(e)}_\varepsilon\boldsymbol{\varepsilon}^{(e)}. \tag{12}$$

Here, $\boldsymbol{d}^{(e)}$ is the rigid displacement and rigid rotation at point $\boldsymbol{x}^p = (x_p, y_p) \in \Omega^{(e)}$, and $\boldsymbol{\varepsilon}^{(e)}$ is a constant strain in the subdomain $\Omega^{(e)}$.

In the case of a two-dimensional problem, the coefficients in Eq. (12) are as follows:

$$\boldsymbol{d}^{(e)} = \lfloor u^p, v^p, \theta^p \rfloor^t, \boldsymbol{\varepsilon}^{(e)} = \lfloor \varepsilon_x, \varepsilon_y, \gamma_{xy} \rfloor^t, \tag{13}$$

$$\boldsymbol{N}^{(e)}_d = \begin{bmatrix} 1 & 0 & -(y-y_p) \\ 0 & 1 & (x-x_p) \end{bmatrix}, \tag{14}$$

$$\boldsymbol{N}^{(e)}_\varepsilon = \begin{bmatrix} x-x_p & 0 & (y-y_p)/2 \\ 0 & y-y_p & (x-x_p)/2 \end{bmatrix}. \tag{15}$$

Here, u^p and v^p represent rigid displacements at point $\boldsymbol{x}^p$ in a subdomain; θ^p represents rigid rotation; and ε_x, ε_y, and γ_{xy} represent the constant strains in the subdomain.

We obtain the following discretized equation:

$$\boldsymbol{K}\boldsymbol{U} = \boldsymbol{P}, \tag{16}$$

where

$$\boldsymbol{K} = \sum_{e=1}^{M}\boldsymbol{K}^{(e)} + \sum_{s=1}^{N}\boldsymbol{K}_{<s>}, \boldsymbol{P} = \sum_{e=1}^{M}\boldsymbol{P}^{(e)}. \tag{17}$$

The discretized equation of the HPM is thus transformed into the simultaneous linear equation of Eq. (16) (Mihara and Takeuchi, 2008). The coefficient matrix of $\boldsymbol{K}$ on the left-hand side can be obtained to assemble each stiffness matrix of the subdomain $\boldsymbol{K}^{(e)}$ and the subsidiary condition on the boundary $\boldsymbol{K}_{<s>}$. Discontinuous phenomena such as opening can be expressed without changing the degrees of freedom by setting the right-hand side of Eq. (11) to zero.

Implementation of Constitutive Model of Reinforced Concrete

Constitutive Law for Compressive Stress of Concrete Material

A typical compressive stress–strain relationship for concrete is shown by the dashed line in Fig. 3. The stiffness gradually degrades with increasing stress up to the compressive strength f_c. After the stress exceeds f_c, softening occurs. The solid line in Fig. 3 represents a trilinear approximation for the skeleton curve, which was also adopted in the RBSM by Takeuchi *et al.* (2005).

An origin-oriented model was adopted for the unloading path, as shown in Fig. 4.

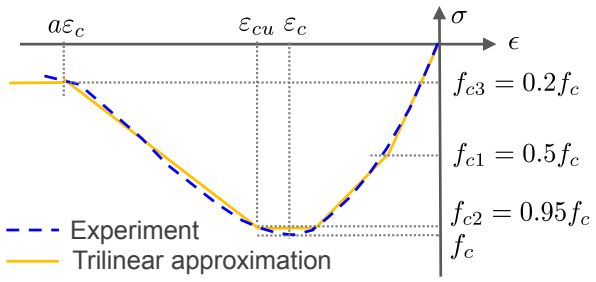

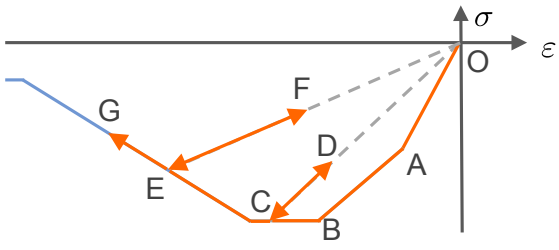

Figure 3. Skeleton curve of compressive stress Figure 4. Hysteresis rule in compressive stress

Constitutive Law for Tensile Stress of Concrete Material

The HPM can separate two subdomains by simply eliminating the penalty. This feature is suitable for representing a discrete crack in concrete. When the surface force σ_n at boundary $\Gamma_{<ab>}$ reaches tensile failure strength f_t, the penalty can then be eliminated, and the discrete crack can be computed as shown in Fig. 5.

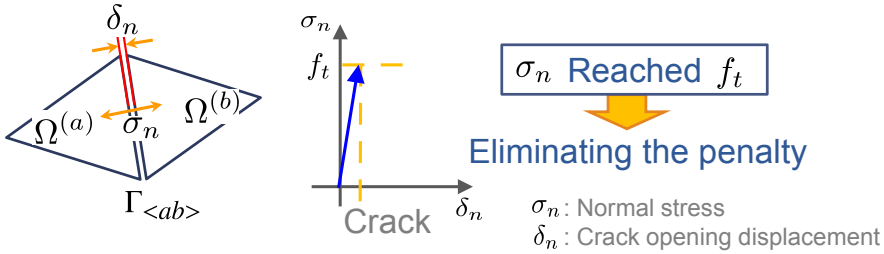

Figure 5. Surface force and tensile strength

The stress in the concrete gradually decreases as the crack opening displacement increases once the tensile failure is exceeded. This behavior is called tension softening. Hilerborg *et al.* (1976) introduced the fracture energy for this tensile softening behavior in a fictitious (or cohesive) crack model. The fracture energy G_f is the area enclosed by the tension-softening curve, and it has a unique value that represents the strength of a concrete material with tensile strength f_t. In the HPM, the tension-softening curve is defined as the relation between the normal stress σ_n and the crack opening displacement δ_n, as shown in Fig. 6.

Many institutes and universities have conducted numerous tests in an effort to obtain the tension-softening curve and fracture energy G_f. In a Technical Committee Report, published by the Japan Concrete Institute (JCI) (2001), on a test method for the fracture property of concrete, several

institutes and universities reported the round-robin results of a three-point bending test on a notched beam. The thin lines in Fig. 7 indicate the results of these tests. For the HPM, we applied a tension-softening curve that corresponds to these test results.

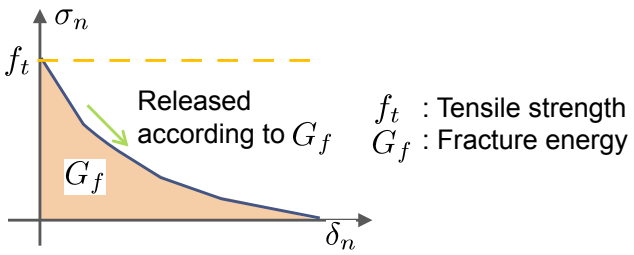

Figure 6. Tension-softening curve for concrete

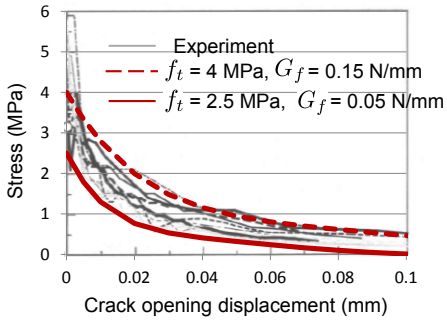

Figure 7. Test results of tension-softening curve (after JCI 2001)

Nakamura *et al.* (1999) compared many empirical derivations of the tension-softening curve and determined that the empirical expression given by Hordijk *et al.* (1986) (Eq. (18)) matched well with past experiments; they used the following expression as a standard for comparison:

$$\frac{\sigma}{f_t} = \left(1 + 27\left(\frac{w}{w_c}\right)^3\right) exp\left(-6.93\frac{w}{w_c}\right) - 28\frac{w}{w_c} exp\,(-6.93), \tag{18}$$

where w is the crack opening displacement (mm), and w_c is the limit virtual crack opening displacement (mm) when the tensile stress is zero; this is given by

$$w_c = 5.14 G_f / f_t, \tag{19}$$

where f_t is the tensile strength (MPa) and G_f is the fracture energy (N/mm).

Equation (18) was adopted to obtain the tension-softening curve in the present study because it corresponded better to the test results than the other proposed empirical expressions.

The thick lines in Fig. 7 are examples of tension-softening curves obtained from Eq. (18). The thick dashed line represents the curve for tensile strength f_t = 4.0 MPa and fracture energy G_f = 0.15 N/mm, and the thick solid line corresponds to f_t = 2.5 MPa and G_f = 0.05 N/mm. Almost all test results fell in the region between these two curves. Therefore, we can conclude that Eq. (18) can represent various materials in concrete.

The origin-oriented model was used for the unloading paths of tensile and compressive stresses.

Thus, stresses and displacements that occur after crack initiation can be calculated accurately because the fracture energy is determined directly.

Constitutive Law for Reinforcing Bar

The reinforcing bar was implemented using layered elements. Fig. 8 shows a schematic image of the layered element for reinforced concrete. The element consists of a concrete layer and arbitrary reinforced bar layers. The layer of a reinforced bar was modeled using a spring element identical to that used in the RBSM. The stiffness matrix for the penalty at the intersection boundary $\Gamma_{<ab>}$ is obtained as follows:

$$\boldsymbol{k}_{<ab>} = p\boldsymbol{k}_{c<ab>} + \sum_{i=1}^{n} \boldsymbol{k}_{si<ab>}, \tag{20}$$

where p is the penalty value, $\boldsymbol{k}_{c<ab>}$ is the stiffness matrix of the concrete material, $\boldsymbol{k}_{si<ab>}$ is the stiffness matrix of the i-th layer of the reinforced bar, and n is the number of reinforced layers.

$\boldsymbol{k}_{si<ab>}$ is obtained from the following relationship between traction and relative displacement at the intersection boundary:

$$\begin{Bmatrix} \sigma_n \\ \tau_s \end{Bmatrix} = \frac{E_s}{h} \begin{bmatrix} \cos^2\theta + \beta \sin^2\theta & (\beta - 1)\cos\theta \sin\theta \\ (\beta - 1)\cos\theta \sin\theta & \sin^2\theta + \beta \cos^2\theta \end{bmatrix} \begin{Bmatrix} \delta_n \\ \delta_s \end{Bmatrix}, \tag{21}$$

where σ_n and τ_s are normal stress and tangential stress, respectively, at the surface $\Gamma_{<ab>}$; δ_n and δ_s are the relative displacements at the $\Gamma_{<ab>}$; E_s is the Young's modulus of the steel; β is the coefficient of the Dowel effect; h is the length between two adjacent subdomains; and θ is the angle to the normal direction of the surface from the axial reinforcement steel (Fig. 9).

A bilinear model was used to solve for the nonlinearity of the reinforcing bar.

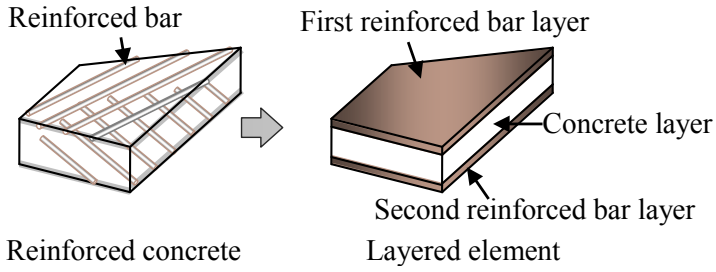

Figure 8. Modeling of reinforced concrete

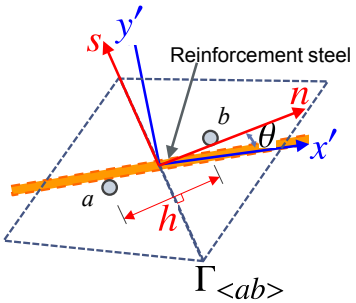

Figure 9. Direction of the steel

Validation

To validate the HPM with a newly implemented reinforced concrete constitutive model, a deep beam test that shows typical progressive failure was simulated.

Description of Deep Beam Test

The crack model was implemented in the HPM to solve a progressive failure problem. This was validated through a simulation of the deep beam test. Details on this experiment were reported by the JCI (1993).

The test model is schematically shown in Fig. 10. The deep beam was placed on steel plates, and a vertical load was applied to the loading plates. The specimen was 900 mm wide, 400 mm high, and 100 mm thick. The specimen was reinforced with six bars.

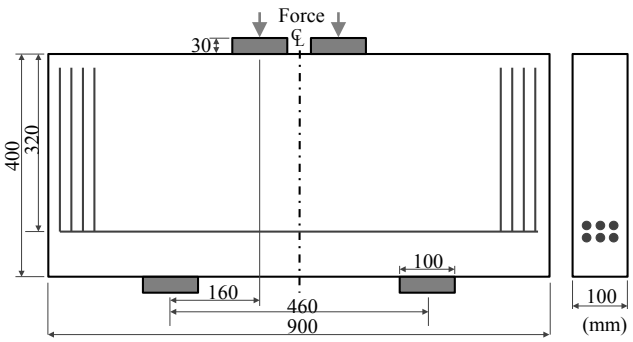

Figure 10. Schematic of test model

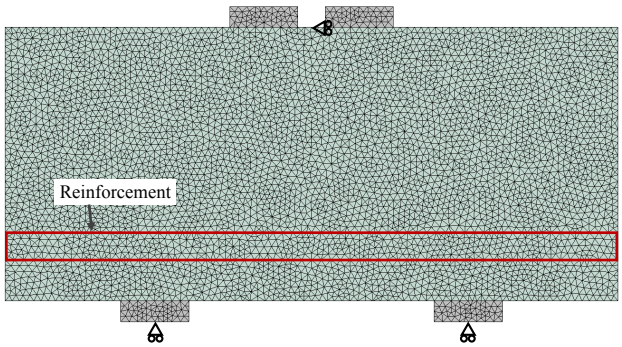

Figure 11. Simulation model

Simulation Model

The simulation model is shown in Fig. 11. The supported point is indicated by a triangular marker. Only the vertical direction was fixed because the concrete block could be rotated during the test. A static load was applied to the top of the plate.

The material properties of the concrete, reinforced layer and steel plates are listed in Table 1. These values were set according to the JCI report (1993).

Yamada's r_{min} method (1968) extended Takeuchi *et al.*'s (2005) method. In the RBSM, this method is used as a nonlinear algorithm that can accurately represent the tensile cracking and compressive failure problems in concrete. This extended r_{min} method was used for the nonlinear algorithm in the present study.

Table 1. Material properties.

(a) Concrete

Parameter	Value
Compressive strength f_c (MPa)	54.4
Tensile strength f_t (MPa)	3.3
Young's modulus E (GPa)	33.3
Poisson's ratio ν	0.167
Thickness (mm)	100.0
Fracture energy G_f (N/mm)	0.13

(b) Reinforcement

Parameter	Value
Young's modulus E (GPa)	210.0
Thickness (mm)	29.79
Angle to the horizontal (°)	0.0
Tensile strength f_t (MPa)	375.3
Coefficient of Dowel effect β	0.005

(c) Steel plate

Parameter	Value
Young's modulus E (GPa)	210.0
Thickness (mm)	100.0
Poisson's ratio ν	0.3

Numerical Results

Figure 12 shows the relationship between the shear force and vertical displacement. The dashed line represents the experimental results, and the solid line represents the numerical results. The numerical results matched well with the experimental results. In the numerical results, a large vertical displacement occurred after the concrete compressive stress under the loading plates reached the compressive strength.

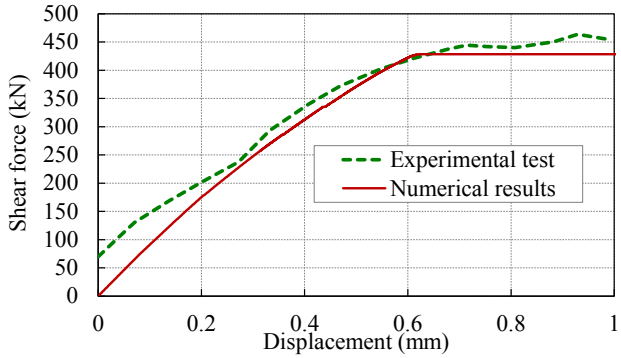

Figure 12. Relationship between shear force and vertical displacement

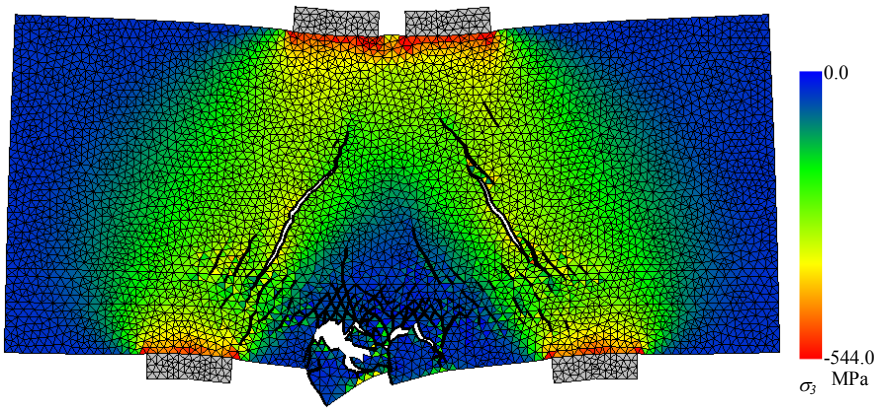

Figure 13. Deformation and contour of minimum principal stress σ_3

Figure 13 shows the numerical deformation (amplification factor 40.0) with a contour of the minimum principal stress σ_3. Multiple progressive cracks propagated from the bottom support steel plate toward the upper loading steel plate in the concrete.

Conclusions

A method to simulate progressive concrete failure was presented and verified using experimental test results. The presented method is an extension of the HPM, in which a constitutive model (discrete crack model) for reinforced concrete is implemented. The discrete crack was evaluated at the intersection boundary between subdomains of the HPM. Simulating the tensile stress behavior and crack displacement is easy; these were directly related to the fracture energy through empirical expressions that were introduced by Hordijk *et al.* (1986). The nonlinearity of the compressive behavior is considered in the compressive stress–strain components of the subdomain of the HPM on the basis of the trilinear approximation function of the empirical stress–strain relationship.

Reinforcing bars were implemented using a layered spring element that is similar to that used in the RBSM. A bilinear model was used to solve for the nonlinearity of the reinforcing bar.

To confirm the validity of the new HPM, we carried out a simulation of a deep beam test. The numerical results were compared with the experimental observations, and we obtained good agreement in the relationship between the shear force and vertical displacement.

Acknowledgments

The experimental results in Figs. 7 and 12 were published in the Committee Report of Japan Concrete Institute (JCI) (2001, 1993).
We extend special thanks to Dr. Ueda for sharing his knowledge of discrete limit analysis and the constitutive model of reinforced concrete.

References

Cornelissen, H. A. W., Hordijk, D. A., and Reinhardt, H. W. (1986), Experiments and theory for the application of fracture mechanics to normal and lightweight concrete. *International Conference on Fracture Mechanics of Concrete.* (Edited by Wittmann, F. H.), Elsevier, Amsterdam.

Fujiwara, Y., Takeuchi, N., Shiomi, T., and Kambayashi, A. (2012), Discrete crack analysis in concrete structure using hybrid-type penalty method. *Proceedings of the 2nd International Conference on Computational Design in Engineering*, 249.

Gedik, Y. H., Nakamura, H., Yamamoto, Y., and Kunieda, M. (2011), Evaluation of three-dimensional effects in short deep beams using a rigid-body-spring-model. *Cement and Concrete Composites*, 33(9–10), pp. 978–91.

Hillerborg, A., Modéer, M., and Petersson, P.-E., (1976), Analysis of crack formation and crack growth in concrete by means of fracture mechanics and finite elements. *Cement and Concrete Research*, 6, pp. 773–782.

JCI (1993), *Application of fracture mechanics to concrete structures.* Japan Concrete Institute, Tokyo.

JCI (2001), Committee report on test method for fracture property of concrete. *Proceedings of the Japan Concrete Institute*, 23, pp. 19–28, (in Japanese).

Kawai, T. (1977), New element models in discrete structural analysis. *Journal of the Society of Naval Architects of Japan*, 141, pp. 187–193.

Mihara, R. and Takeuchi, N. (2008), Nonlinear analysis of Riedel shearing test by using mesh dividing method in HPM. *Proceedings of the 8th International Conference on Analysis of Discontinuous Deformation*: *Fundamentals and Applications to Mining and Civil Engineering*, pp. 201–206.

Nakamura, S., Kitsutake, Y., Mihashi, H., and Uchida, Y. (1999), Discussion on standard evaluation method for tension softening properties of concrete. *Concrete Research and Technology*, 10(1), pp. 151–164 (in Japanese).

Rice, J. R. (1968), Path independent integral and the approximate analysis of strain consideration by notches and cracks. *Journal of Applied Mechanics*, 35, pp. 379–386.

Takeuchi, N., Ueda, M., Kambayashi, A., and Kito, H. (2005), *Discrete limit analysis of reinforced concrete structure*, Maruzen, Tokyo (in Japanese).

Takeuchi, N., Tajiri, Y., and Hamasaki, E. (2009), Development of modified RBSM for rock mechanics using principle of hybrid-type virtual work. *Analysis of Discontinuous Deformation: New Developments and Applications*, (Ma, G. and Zhou, Y.). pp. 395–403, Research Publishing Service, Singapore.

Yamada, Y., Yoshimura, N., and Sakurai, T. (1968), Plastic stress–strain matrix and its application for the solution of elasto-plastic problem by a finite element method. *International Journal of Mechanical Sciences*, 10, pp. 343–354.